Laser offset-frequency locking up to 20 GHz using a low-frequency electrical filter technique

Stephane Schilt,[1,2,*] Renaud Matthey,[3,4] Daniela Kauffmann-Werner,[1,6] Christoph Affolderbach,[5] Gaetano Mileti,[5] and Luc Thévenaz[1]

[1]Ecole Polytechnique Fédérale de Lausanne (EPFL), Institute of Electrical Engineering, STI-GR-SCI Station 11, CH-1015 Lausanne, Switzerland

[2]Now at IR Microsystems SA, PSE-C, CH-1015 Lausanne, Switzerland

[3]Observatoire Cantonal de Neuchâtel, Rue de l'Observatoire 58, CH-2000 Neuchâtel, Switzerland

[4]Now at Centre Suisse de Microtechnique et d'Electronique, CSEM SA, CH-2000 Neuchâtel, Switzerland

[5]Université de Neuchâtel, Laboratoire Temps—Fréquence (LTF), Rue A.-L. Breguet 1, CH-2000 Neuchâtel, Switzerland

[6]Now at Institut für Strahlwerkzeuge (IFSW), Stuttgart University, D-70569 Stuttgart, Germany

*Corresponding author: schilt@ir-microsystems.com

Received 22 February 2008; revised 2 July 2008; accepted 8 July 2008; posted 15 July 2008 (Doc. ID 92918); published 15 August 2008

A simple, easy-to-implement, and robust technique is reported to offset lock two semiconductor lasers with a frequency difference easily adjustable up to a couple of tens of gigahertz (10 and 19 GHz experimentally demonstrated). The proposed scheme essentially makes use of low-frequency control electronics and may be implemented with any type of single mode semiconductor laser, without any requirement for the laser linewidth. The technique is shown to be very similar to the wavelength modulation spectroscopy method commonly used for laser stabilization onto molecular absorption lines, as demonstrated by experimental results obtained using 935 nm laser diodes. © 2008 Optical Society of America

OCIS codes: 140.3425, 300.6360, 300.6380, 140.3518, 140.5960, 120.4800.

1. Introduction

Accurate control of the emission frequency of one or several lasers is required in a variety of fields, such as in advanced optical fiber telecommunications, in time and frequency standards (atomic clocks), or in high resolution atomic and molecular spectroscopy. In all these applications, a precisely defined optical frequency is needed and long-term stability must be ensured for correct system operation, with a required degree of stability and accuracy that depends on the application. Semiconductor laser diodes are highly suitable laser sources for such applications, thanks to their unique properties such as compactness, robustness, low power consumption, high spectral purity, and long lifetime, but they usually require active stabilization to secure proper medium- and long-term frequency stability (fractional frequency stability of 10^{-7} or better). A proven technique for this purpose is to lock the laser frequency on a molecular or atomic absorption line, as already demonstrated in a large part of the optical spectrum ranging from the visible to the midinfrared [1–6]. Here we present an original and efficient technique to lock two semiconductor lasers at a fixed frequency difference up to many tens of gigahertz, combining simplicity and flexibility and essentially relying on low-frequency control electronics.

So far, one of the most common techniques to realize such stabilization is based on wavelength modulation spectroscopy (WMS) [7,8], in which the wavelength of the laser is dithered through a modulation of its injection current. Line-locking schemes

0003-6935/08/244336-09$15.00/0

based on WMS show the disadvantage that only discrete specific reference frequencies may be used, since they must coincide with an absorption line of sufficient strength but offer the advantage that the precise obtained laser frequency does not vary if the strength of the reference absorption line changes. Locking to the side of an absorption line (side locking) with a dual-detector configuration [2,5] does not involve any laser modulation but still limits the locking range to the neighborhood of an atomic or molecular absorption line. Furthermore, the precise frequency of the locked laser moves when the strength of the reference line changes. However, some applications require the stabilization of a laser source at a frequency located away from any absorption line, which cannot be accomplished using the above-mentioned techniques. This is, for example, the case in the differential absorption lidar (DIAL) technique for which one or several on-line wavelengths as well as one off-line wavelength must be precisely controlled and stabilized [3,9].

Frequency control of the off-line laser is generally accomplished by stabilizing a so-called slave laser relative to a stable reference such as another directly stabilized laser (labeled the master laser), at a precise frequency difference, which is referenced as offset locking. Among various methods proposed so far to realize offset locking, one of the most exploited techniques makes use of an optical phase-locked loop (OPLL) to secure phase coherence between the two lasers [10]. Yet, a high bandwidth of the overall control loop electronics is required in this approach to ensure that phase fluctuations of the optical sources are accurately canceled [11]. Therefore, either very narrow linewidth lasers, such as external cavity laser diodes (ECLDs), or extremely short loop delay times, in the picosecond region, are required for successful phase locking, which makes this technique difficult to be implemented in a more general situation, such as experienced using distributed feedback (DFB) lasers with a typical linewidth of a few megahertz or above.

In many applications phase coherence between the two offset-locked lasers is however not necessary, and an optical frequency lock loop is often sufficient, which drastically alleviates the bandwidth requirement on the control electronics. Here we report on a simple technique to realize frequency offset locking between two lasers. The proposed method is an alternative of the modulation-free filter technique presented by Ritt *et al.* [12]. By adding modulation to one of the lasers, we were able to generate an error signal that is very similar to the signal used in WMS for on-line laser stabilization to a molecular absorption feature. Besides its simplicity, the main advantage of this method is to essentially use low-frequency electrical components (apart from a fast photodetector and a frequency downconversion stage) to achieve offset frequencies up to several tens of gigahertz (20 GHz experimentally demonstrated). This offset-locking scheme has been developed for the realization of a multiple-frequency reference unit to be used for future injection seeding in a four-wavelength spaceborne water vapor DIAL system operating in the 935 nm range [9]. In the following, we present a detailed description of the offset-locking principle, including both simulations and experimental demonstrations. The offset-locking scheme was primarily implemented to operate at 18.79 GHz offset frequency in the developed frequency reference unit, but the reported principle is extendable to any frequency difference up to several tens of gigahertz by properly extending the photodetector bandwidth.

2. Description of the Offset-Locking Scheme

A. Principle

The basic principle of the reported offset-locking scheme consists in controlling the frequency difference between the master and the slave lasers, which requires as a first step to detect the beat-note signal between the two lasers using a high-bandwidth photodetector. The stabilization is then realized using a low-bandwidth electrical filter acting as a frequency discriminator. The idea is to use the filter in combination with other low-frequency electrical components as schematically depicted in Fig. 1 to create a so-called artificial reference line in the electrical (low-

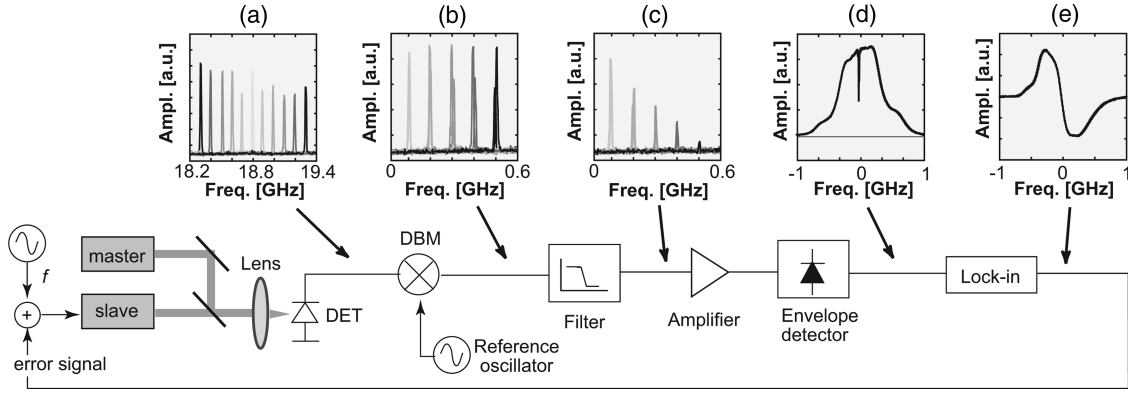

Fig. 1. Scheme of the offset-locking setup: DET, high-bandwidth photodiode; DBM, double-balanced mixer. A summary of the signals experimentally measured at different stages of the system is also displayed in (a)–(e). The signals given in different gray levels in (a)–(c) refer to different master–slave frequency detunings.

frequency) domain, to which the beat-note frequency is locked, in analogy to the molecular absorption lines in the optical domain used in WMS. For this purpose, the beat-note signal from the photodetector is first combined with a reference signal delivered by a frequency generator or by a dielectric resonator oscillator (DRO) in a double-balanced mixer for frequency downconversion. These elements are the only high-frequency components used in our setup, with all other components operating in the low-frequency range. This constitutes a major advantage of the reported technique compared to OPLL-based methods, which require a high bandwidth of the entire electronic system. As a result, the reported method is straightforwardly applicable to DFB lasers at high offset frequency, which does not arise for OPLLs [11]. The mixer intermediate frequency is then filtered and possibly amplified to secure proper operation of the offset-locking scheme even in the case of very weak beat signals. Finally, the power of the radio frequency signal is measured using an envelope detector. When the beat-note frequency is modulated (through wavelength dithering of one of the lasers, for instance, by injection current modulation in a semiconductor laser), derivatives of the filter transfer function are obtained at the harmonics of the modulation frequency in the same way as in WMS for a molecular absorption line. The first harmonic signal is used as an error signal in a regulation loop to control the slave laser frequency to lock the mixer intermediate frequency to the center of the filter. The use of a narrow filter with steep slopes enables the efficient stabilization of the beat frequency at the target offset frequency. Either a low-pass or a bandpass filter may serve to create the artificial line. In the first case, the reference frequency f_{ref} applied to the mixer for the frequency downconversion coincides with the offset frequency f_{offset}, whereas $f_{\mathrm{ref}} = f_{\mathrm{offset}} \pm f_{\mathrm{filter}}$ in the second case, where f_{filter} is the center frequency of the bandpass filter.

B. Electrical Filter for the Offset-Locking Scheme

The main difference between the use of a bandpass or a low-pass filter in the reported offset-locking scheme is related to the number of different operating locking points. A disadvantage of the use of a bandpass filter is the nonuniqueness of the locking point. In fact, four different locking points can be set as illustrated in Fig. 2. A twofold degeneracy occurs as the sign of the beat-note frequency is undetermined, i.e., it is not possible to distinguish between the two cases $\nu_M - \nu_S = \pm f_{\mathrm{offset}}$, where ν_M and ν_S are the optical frequencies of the master and slave lasers, respectively. However, these two locking points are generally far from each other (twice the offset frequency), so this does not really cause a problem in practice. It should be pointed out that this ambiguity always occurs when the beat-note signal is used (this is also the case for OPLLs). However, a second ambiguity also occurs, due to the impossibility to determine the sign of the intermediate frequency $f_{\mathrm{beat}} - f_{\mathrm{ref}}$, which leads to two possible locking points at $f_{\mathrm{beat}} - f_{\mathrm{ref}} = \pm f_{\mathrm{filter}}$. These two points are much closer (only 2 GHz if a 1 GHz bandpass filter is used), which can lead to an incorrect locking point. Improvement of the technique may be achieved using a low-pass filter instead of a bandpass. A low-pass filter presents a symmetric shape similar to a bandpass filter when negative frequencies are considered, but centered on zero. With such a filter, the intermediate frequency is stabilized around zero, which removes the ambiguity on the locking point ($f_{\mathrm{beat}} = f_{\mathrm{ref}} \pm f_{\mathrm{filter}} = f_{\mathrm{ref}}$ as $f_{\mathrm{filter}} = 0$). Another advantage offered by the use of a low-pass filter is an improved thermal stability: whereas the center frequency of a bandpass filter can slightly drift with temperature, it remains zero for a low-pass filter (even if the cutoff frequency slightly changes with temperature). The center frequency of the filter artificial line is thus intrinsically stable, so that the absolute stability of the offset-locked laser is only limited by the stability of

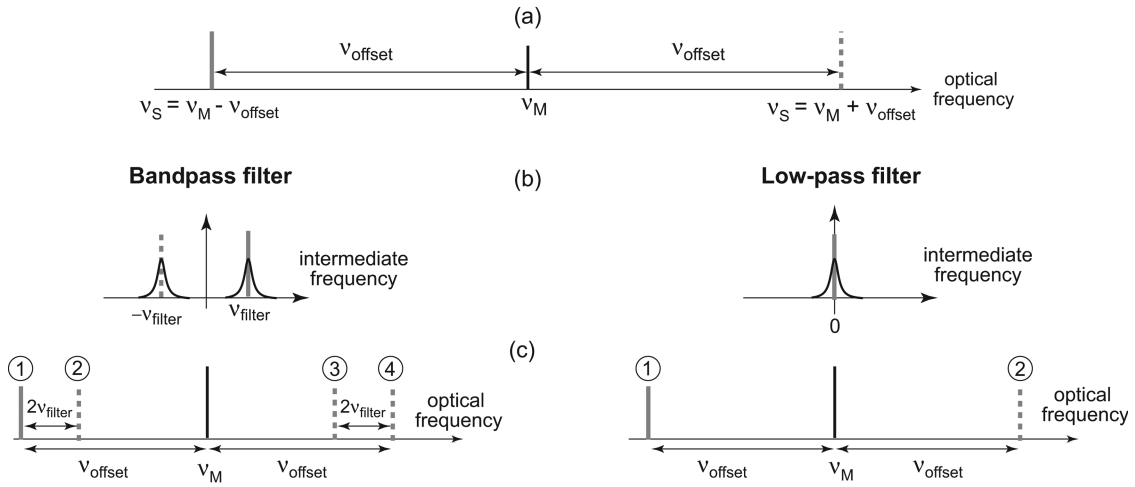

Fig. 2. Degeneracy obtained for (a) the beat signal, (b) the intermediate frequency signal, and (c) the laser locking point for a bandpass and a low-pass electrical filter.

the reference microwave signal (which can be as low as <100 kHz) and by the stability of the master laser. Therefore, we consider here only the case of a low-pass filter, as it provides a more robust scheme.

C. Simulations of the Harmonic Signals

Simulations have been performed to determine the shape of the harmonic signals obtained when the frequency of the beat-note signal between the two lasers is modulated at frequency f. The simulations consider the interaction of the frequency modulated beat-note signal with an electrical filter modeled by its transfer function, in a similar way as done in WMS for the interaction of the modulated optical frequency with a molecular absorption line [8,13]. Likewise, a normalized frequency modulation index m is introduced, defined as the frequency excursion Δf_{beat} of the beat-note signal normalized to the full width at half-maximum (FWHM) of the filter spectral response Δf_{filter}: $m = \Delta f_{\text{beat}}/\Delta f_{\text{filter}}$. Whereas analytical expressions of the harmonic signals can be obtained in WMS for a Lorentzian absorption line shape probed by a laser with a combined intensity modulation (IM) and wavelength modulation (WM) [8], this is not possible for the more general transfer function describing the filter response. Therefore, numerical calculations were performed based on a FFT algorithm to extract the first harmonic components resulting from the interaction of the beat signal with the filter. The residual IM of the slave laser was also considered in the model with an arbitrary IM-WM phase shift. Low-pass filters of different orders can be considered in the simulations, but a first order low-pass filter with a cutoff frequency of 220 MHz has been used in the present case for simplification and for comparison with experimental conditions. Results for the three first harmonics are displayed in Fig. 3. It clearly appears that the harmonic signals look like successive derivatives of the filter function and are very similar to the signals obtained in WMS for a molecular absorption line. This analogy will be discussed in more detail in Section 3.

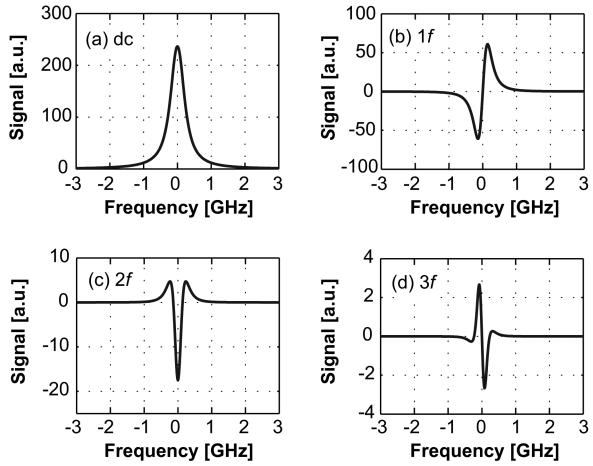

Fig. 3. (a) Simulation of the filter response curve and (b)–(d) of the three first harmonic signals obtained for a low-pass filter with 220 MHz cutoff frequency and for a modulation index $m = 0.4$.

3. Experimental Results

A. Implementation of the Offset-Locking Scheme

Two 935 nm semiconductor lasers have been used for the implementation of the offset-locking technique schematically depicted in Fig. 1. The master laser was a homemade ECDL developed at the Observatory of Neuchâtel [14], with typical characteristics of 30–40 mW output power, 0.3 MHz linewidth, 35 nm overall tunability and mode-hop-free tuning range larger than 10 GHz. This laser can be stabilized to a water vapor absorption line using a WMS scheme with a suitable reference cell filled with low-pressure H_2O [9]. The slave laser was a DFB laser from Nanoplus GmbH (Germany) with 10 mW output power. A 40 mm focal length achromat lens focuses the two superimposed laser beams on a small area (25 μm diameter) 25 GHz photoreceiver (New-Focus 1437 M). A double balanced mixer (Miteq DM0520LW1) and a reference signal from a 18.79 GHz DRO (Miteq, DRO-K-18791-ST) or from a frequency-variable function generator (HP 8673H) are used for frequency downconversion. The artificial reference line for offset locking is realized with an electrical low-pass filter (Mini-Circuit VLF225) with a measured 3 dB cutoff frequency around 220 MHz, yielding to a corresponding microwave feature of 440 MHz (FWHM), to be compared with the typical 1.2 GHz Doppler width (FWHM) of a water absorption line in this spectral range. This width could be easily reduced using a lower cutoff frequency filter when required, but in most cases the stability requirements for the off-line laser are less stringent than for the master laser, and the selected filter was by far narrow enough in our experiments. A 50 dB high-gain amplifier (Miteq, AM-1309) secures proper operation of the offset-locking scheme even in the case of very weak beat signals. Finally, an envelope detector (Herotek, DHM124AA) realizes the AM demodulation. Note that the use of the low-pass filter results in a transmission feature rather than an absorption feature, as is the case in molecular absorption spectroscopy. However, the resulting $1f$ error signals are completely equivalent in the two cases.

Figure 1 also displays a summary of the signals experimentally observed at the different stages of the offset-locking scheme, from the beat signal at the output of the fast detector 1(a), frequency downconverted 1(b), and filtered 1(c), to the filter frequency response obtained when scanning the beat-note frequency 1(d), and finally the derivative error signal used for laser stabilization 1(e).

The modulation of the beat signal was performed in our experiments by modulating the current of the slave laser at a frequency of 50 kHz but it could also be equivalently implemented through a modulation of the master laser. The error signal was fed back to the slave laser through a PI regulator loop to maintain the frequency difference between the two lasers

at the target offset value. For the characterization of the error signal, the current of the master laser was additionally ramped at a low frequency (16 Hz) to sweep the beat signal through the microwave artificial line, and the 1f signal was recorded on an oscilloscope during the scan. The error signal has been observed in different conditions, and its evolution has been investigated as a function of the main experimental parameters, such as the laser modulation depth, the phase of the lock-in detection, and the optical power coupled onto the detector.

Figure 1(d) illustrates the artificial reference line generated by the filter during the slow scan of the master laser wavelength (in the absence of modulation). It has an approximate width of 440 MHz (FWHM) and no signal is transmitted outside a 1 GHz window (±500 MHz). The line presents an asymmetric shape, which probably results from the variation of the beat signal amplitude induced by the applied current ramp or from the not totally flat frequency response of the photodetector. The narrow dip in the center of the line is induced by the amplifier used to enhance the signal, which has a nonzero low-frequency cutoff. Ideally, an amplifier with a bandwidth starting at DC level should be used, whereas the amplifier implemented here has a low cutoff frequency of 10 kHz. The frequencies below 10 kHz are thus less amplified, which generates the narrow dip in the artificial line. In principle, this dip could be used as a very narrow line for frequency locking. But this was not practically applicable, since such a small laser WM amplitude would be required that the resulting 1f signal would not have been detectable in our experimental conditions. Instead, the wider filter transfer function was used for frequency locking, in conjunction with a larger WM amplitude ranging from 0.1 to 3.5 times the filter width. In such conditions, the influence of the narrow dip is removed and a smooth derivative signal is obtained; see Fig. 1(e). The normalized filter response (without the narrow central dip) is compared in Fig. 4 with the theoretical shape corresponding to a first order low-pass filter with an identical cutoff frequency of 220 MHz, as applied in the simulations. A discrepancy between the experimental shape and the curve considered in the simulations is noticed, which will contribute to the quantitative differences observed between simulated and experimental 1f signals as shown later.

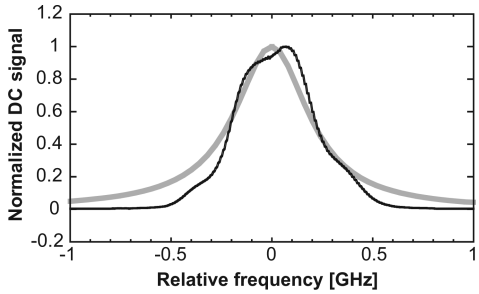

Fig. 4. Comparison of the normalized response of the filter experimentally measured (black thin curve) and considered in the simulation model (gray thick curve).

B. Influence of the Modulation Amplitude on the 1f Signal

The error signal has been measured as a function of the modulation index m and has been compared to simulations as shown in Fig. 5. The observed behavior is very similar to the situation experienced when a molecular absorption line is probed by a wavelength-modulated laser [8]. A derivativelike signal

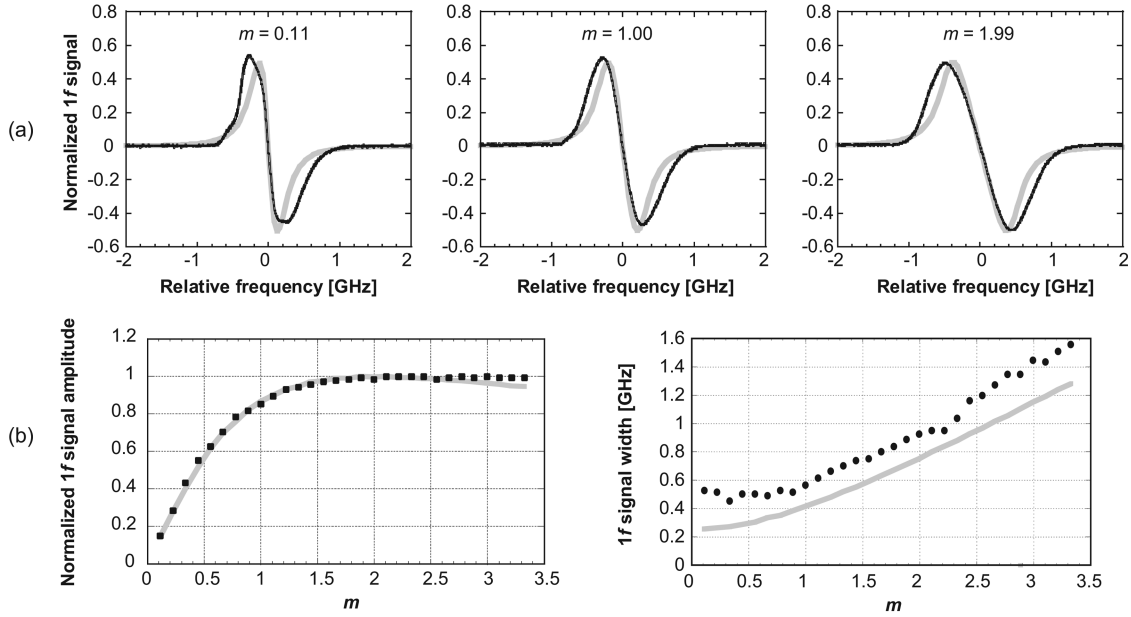

Fig. 5. (a) Normalized 1f signals obtained experimentally (black thin curves) and from simulations (gray thick curves) for different values of the modulation index m. The normalization is made so that the maximum signal amplitude corresponds to one for both experimental and simulations curves. (b) Amplitude and width (distance between maximum and minimum) of the normalized 1f signal as a function of the modulation index m.

is generated, whose amplitude and width depend on the modulation index. A good general qualitative agreement is obtained between experimental and simulated signals, particularly regarding the evolution of the $1f$ signal amplitude with respect to m. However, discrepancies are observed when looking more quantitatively at the results, especially about the precise shape of the $1f$ signal. This is likely due to the difference between the real filter response curve and the theoretical function considered in the simulations. In particular, the calculated curve is slightly narrower than the real response in the central part of the profile (see Fig. 4), which leads to narrower simulated $1f$ signals compared to the experimentally measured. As in the case of a molecular absorption line [13], the signal of maximum amplitude is reached for $m \cong 2$.

The $1f$ signals displayed in Fig. 5(a) show a smooth derivative shape even for modulation indices as low as $m = 0.1$. For such modulation conditions, the narrow dip that was observed in the direct output signal of the offset-locking scheme does not affect the $1f$ signal, as previously discussed.

C. Influence of the Detection Phase on the $1f$ Signal

The variation of the error signal with respect to the lock-in detection phase is shown in Fig. 6 and is compared to simulations. Good qualitative agreement is observed, but quantitative discrepancies occur for the same reason as previously mentioned. Here again, the observed behavior is very similar to the situation experienced when a molecular absorption line is probed by a wavelength-modulated laser: the amplitude of the $1f$ signal varies periodically with the phase Φ_1 of the lock-in detection and the signal of maximum amplitude is obtained for $\Phi_1 = \Psi$ as in WMS, where Ψ is the IM-WM phase shift [15]. The only but important difference is that the $1f$ signal is free from background offset for any detection phase, whereas such a background offset is usually present in the $1f$-WMS signal as a result of the laser residual IM occurring when the current of a semiconductor laser is modulated [16]. Here, the out-of-resonance IM-induced offset is absent because there is strong signal suppression by the low-pass filter outside its bandwidth. Additionally, the strength of the attenuation induced by the filter is much stronger than the absorption usually produced by a molecular absorption line (using a reasonable path length), so that the offset at line center, even if it would exist, would be very small compared to the strength of the filter $1f$ signal and is thus negligible. Therefore, the offset-locking scheme behaves like a molecular absorption line probed by pure WM. This property is positive for laser frequency stabilization, as the detection phase Φ_1 may be adjusted to maximize the amplitude of the $1f$ signal ($\Phi_1 = -20°$ in the present case, corresponding to the IM-WM phase shift in the modulated slave laser). Such an adjustment is not possible in the general case of WMS as the detection phase needs to be tuned to cancel the offset level, which usually reduces the amplitude of the error signal compared to its maximum value.

D. Influence of the Optical Power on the Error Signal

The dependence of the error signal toward the optical power focused on the detector has been measured by changing the incident power from the master and slave lasers using several optical attenuators with different attenuation factors. The relevant parameter for the amplitude of the beat signal is the power of the interference component, which is proportional

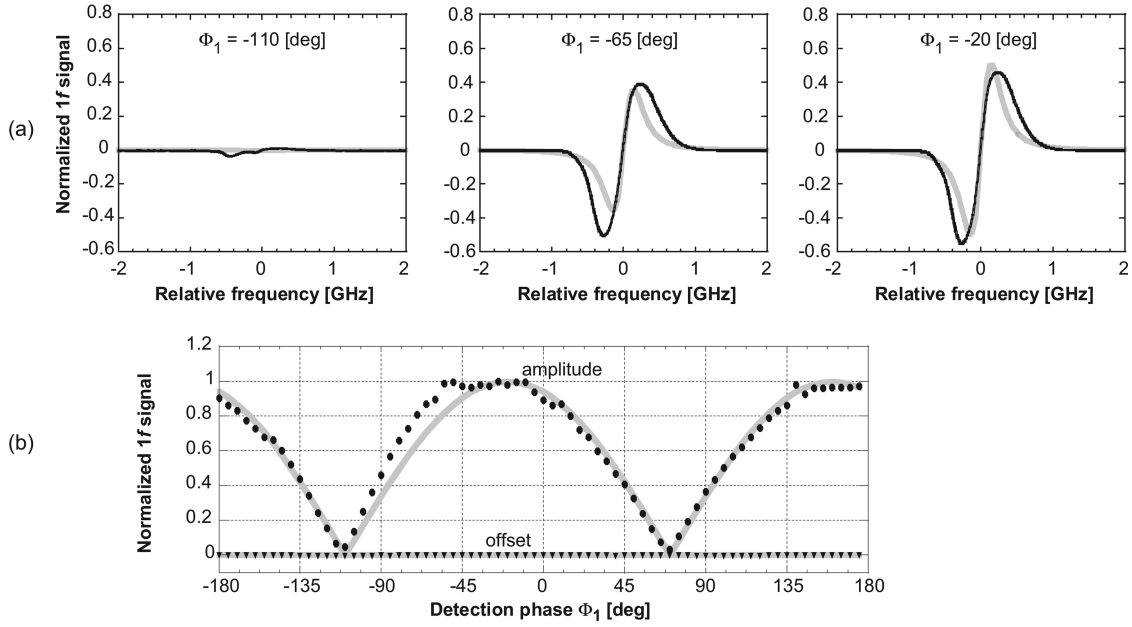

Fig. 6. (a) Normalized $1f$ signals obtained experimentally (black thin curves) and from simulations (gray thick curves) for different values of the detection phase Φ_1. The normalization is made so that the maximum signal amplitude corresponds to one for both experimental and simulations curves. A modulation index $m = 0.44$ has been considered. (b) Amplitude and offset of the normalized $1f$ signal as a function of the detection phase. The offset represents the out-of-resonance $1f$ signal level in Fig. 6(a).

to the square root of the product of the optical powers P_M and P_S from the master and slave lasers, respectively. Experimental results are shown in Fig. 7 for different conditions. In a first series of measurements, the optical power of both lasers has been simultaneously changed. In a second series, the power from only one laser has been varied. The error signals corresponding to these different conditions are displayed in Figs. 7(a) and 7(b), respectively. The amplitude of the error signal as a function of the incident optical power is shown in Fig. 7(c).

In Fig. 7(a), a nice error signal is obtained with approximately 1 mW from each laser, but it can even be detected with a good signal-to-noise ratio with an optical power as low as 0.03 mW from each laser. The amplitude of the derivative signal has a good linearity with the amplitude of the interference term. Some small distortions occur in the signal when the optical power is reduced, but they do not prevent laser locking using this signal as an error signal.

E. Experimental Demonstration of the Offset-Locking

Two different experiments have been carried out to demonstrate the suitability of the developed offset-locking technique. In the first one, operation at 10 GHz offset frequency was investigated. Two strong H_2O absorption lines separated by 9.5 GHz around 10683.5 cm^{-1} have been used to quantify the absolute stability of the offset-locked laser. For this purpose, the master laser was stabilized onto one of these strong H_2O lines using a WMS scheme with a 4 m path length multipass cell filled with 22 mbar H_2O [see Fig. 8(a)]. The slave laser was offset locked by 10 GHz from the master. The second H_2O line was used as a frequency discriminator to evaluate the absolute stability of the offset-locked laser. A 500 MHz shift was considered in addition to the 9.5 GHz separation of the two lines in order that the slave laser wavelength lies on the slope of the second H_2O line [see Fig. 8(b)]. The direct absorption signal from a 22 cm long cell filled with 22 mbar pure H_2O used in a double-path configuration (thus providing a 44 cm path length) served as a measurement of the slave laser absolute frequency. In addition, a high precision wavemeter (HighFinesse WS/Ultimate, with an absolute accuracy of 10 MHz) was used to monitor the master laser wavelength.

The frequency deviation of the two lasers continuously measured during more than 1 day is shown in Fig. 9. It may be observed that each single frequency change of the master laser, even small, is reflected in the slave laser frequency. We attribute the sawtooth-like structure observed in the frequency evolution of both lasers to residual frequency instabilities of the locked ECDL master laser caused by etalon fringes or other temperature-related effects in the setup.

A second experiment was performed to demonstrate the offset-locking operation at 18.79 GHz offset frequency at the precise wavelength considered in the multiple-frequency reference unit [9]. In that case, the master laser was stabilized onto a weak H_2O absorption line at 10684.83 cm^{-1} using WMS

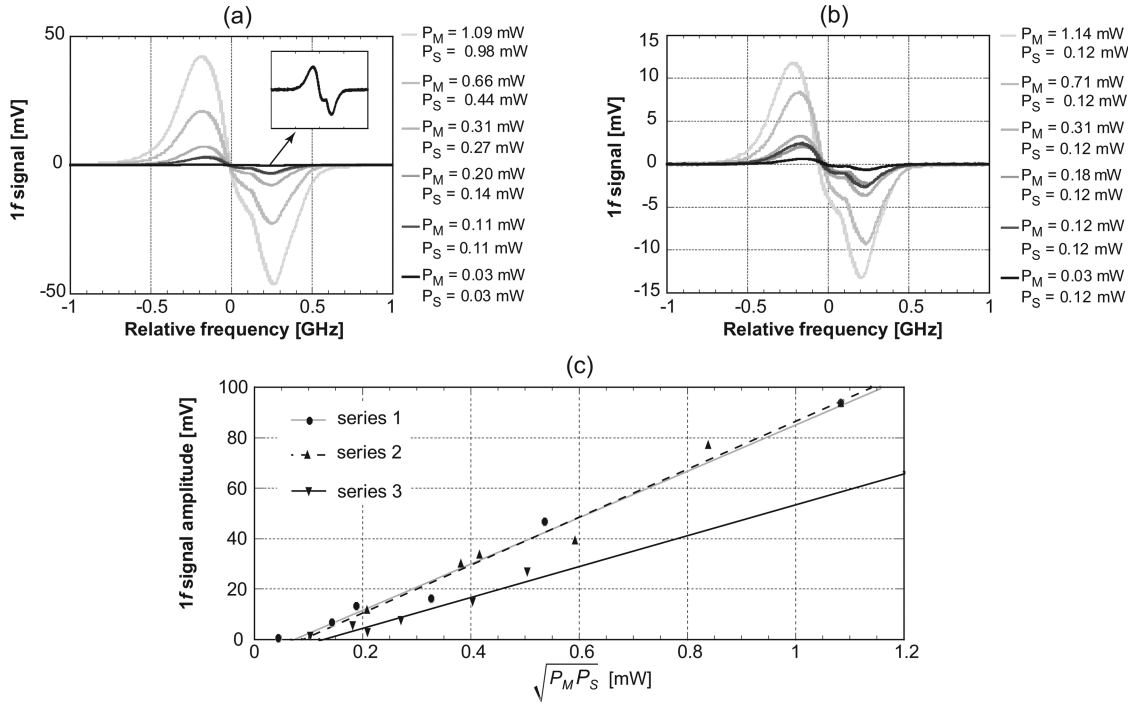

Fig. 7. Error signal obtained for different optical power on the detector. (a) The power from both lasers is simultaneously varied. (b) The power from only one laser (master) is changed, whereas the power from the other laser (slave) is kept constant. (c) Amplitude of the error signal as a function of the optical power. Three series of measurements are displayed: in series 1, the power of both lasers is simultaneously varied; in series 2, the power of the master laser only is changed, whereas the power from the slave laser is kept constant. Series 3 is similar to series 2, but with a much smaller power from the slave laser. All these results have been obtained with a modulation index $m = 0.14$ in the slave laser.

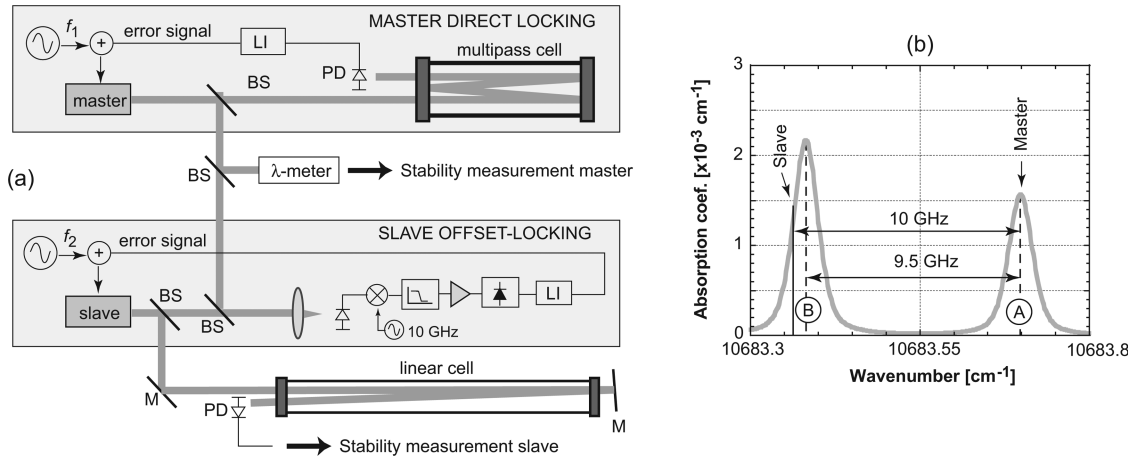

Fig. 8. (a) Scheme of the experimental setup used for the evaluation of the offset-locking technique at 10 GHz offset frequency: BS, beam splitter; M, mirror; PD, photodiode; LI, lock-in. The master laser is stabilized onto a H_2O line at 10683.7 cm^{-1} using WMS with a multipass cell. The slave laser is offset locked 10 GHz away from the master using the offset-locking method. The stability of the lasers is respectively monitored using a high precision wavemeter (master) and a second H_2O line in a linear gas cell (slave). (b) HITRAN simulation of the two H_2O lines (22 mbar pure H_2O) used for the stabilization of the master laser (line A) and as a discriminator to monitor the stability of the slave laser (line B).

and the same 4 m multipath cell as previously. The slave laser was offset locked 18.79 GHz away from the master, out of any H_2O absorption line. Its stability was monitored using the high precision wavemeter (no absorption feature could be used for this purpose since the slave laser was locked off-line). The absolute stability of the master laser was not quantitatively measured in that case, but the error signal used for the stabilization of the master laser onto the H_2O line was monitored as an indicator of the stability of this laser and for comparison with the slave laser behavior analyzed with the wavemeter. The discriminator slope was not quantified, so that this signal gives only a qualitative tendency of the master laser frequency evolution. Additionally, the error signal used in offset-locking regulation loop was also measured as a qualitative representation of the relative stability between the two lasers. Results are shown in Fig. 10. Here again, a parallel evolution of the frequency of both lasers is observable, showing that the slave laser properly tracks the master frequency. Large frequency hops regularly observed in the error signal of both lasers as well as in the wavemeter measurement result from residual frequency instabilities caused by the ECDL master laser locking setup as previously discussed. This phenomenon degrades the absolute stability of both lasers, but constitutes an excellent illustration of the offset-locking performances, showing that the slave laser actually follows any change, even abrupt, of the master laser.

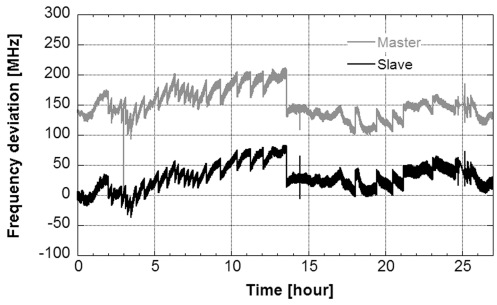

Fig. 9. Evaluation of the stability of the offset-locking scheme at 10 GHz offset frequency, measured with the setup described in Fig. 8. The frequency deviation of both lasers is displayed over more than 1 day with the master laser locked onto a H_2O line.

4. Discussion and Conclusion

A simple but powerful and versatile method has been proposed and demonstrated to realize offset locking between two semiconductor lasers. Besides a fast photodetector, a reference signal at the target offset frequency, and a double-balanced mixer for frequency downconversion, the reported technique makes use of low-frequency electronics but is able to achieve offset locking in a wide range of offset frequency using the same setup. Offset frequencies up to 20 GHz have been demonstrated in this paper, but the technique is immediately extendable to higher frequencies. The offset frequency is simply adjusted by a reference signal at the targeted frequency.

The reported technique performs a relative stabilization of the frequency of the two lasers without relying on phase coherence. The benefit of the technique is that it can be applied to any type of semiconductor lasers without any requirement on the laser linewidth as is the case in OPLL-based techniques. The reported offset-locking scheme is very similar to the WMS technique frequently used in high sensitivity trace gas detection for laser stabilization onto a molecular or atomic absorption line, as shown both by harmonic signals simulations and by experimental data. It can therefore be described by a similar formalism, and the same type of locking electronics can be used. This is a major benefit of the reported technique, since stabilization loop based on WMS for laser locking is a well-known technique that has proved its suitability and reliability for a long time.

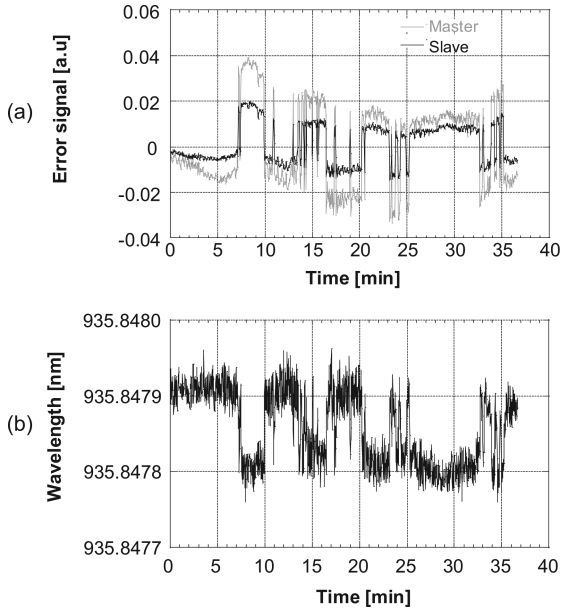

Fig. 10. Evaluation of the stability of the offset-locking scheme at 18.79 GHz offset frequency. (a) Comparison of the error signals of the master and slave lasers, showing their parallel evolution. Large vertical hops regularly observed in both traces result from etalon fringes or other temperature-related effects in the overall optical setup. (b) Absolute stability of the offset-locked slave laser monitored with a high precision wavemeter.

In the reported technique, the electrical filter creates an artificial reference line in the electrical domain, to which the beat-note signal between the master and the slave lasers is stabilized. The use of an accurate frequency reference as provided by a DRO enables us to obtain a precise offset frequency between the two lasers as was previously reported [9]. To achieve an absolute stabilization of the slave laser, the master laser must be locked to an absolute reference such as a molecular absorption line. In that case, the offset-locking scheme has demonstrated its robustness and the absolute stability of the slave laser was limited essentially by the fluctuations of the master laser in our experiments rather than by the relative offset locking between the two lasers. However, the relative stability of the offset-locking scheme is much better and values <100 kHz are straightforwardly achievable since very accurate and stable reference frequencies may be obtained over a large range scaling from one to several tens of gigahertz using DROs (with relative stability of the order of 10^{-5}).

The authors acknowledge the European Space Agency ESA (ESTEC Contract 17267/03/NL/CH), the Ecole Polytechnique Fédérale de Lausanne, the Canton de Neuchâtel, and the Swiss National Science Foundation (projects 2100-066821.01, R'Equip 2160-06749) for their financial support.

References

1. H. Hori, Y. Kitayama, M. Kitano, T. Yabuzaki, and T. Ogawa, "Frequency stabilization of GaAlAs laser using a Doppler-free spectrum of the Cs-D_2 line," IEEE J. Quantum Electron. **QE-19**, 169–175 (1983).
2. F. Bertinetto, P. Gambini, M. Puleo, and E. Vezzoni, "Performance and limitations of laser diodes stabilized to the sides of molecular absorption lines of ammonia," Rev. Sci. Instrum. **64**, 2128–2132 (1993).
3. C. M. Fitzgerald, G. J. Koch, A. M. Bullock, and A. N. Dharamsi, "Wavelength modulation spectroscopy of water vapor and line center stabilization at 1.462 μm for lidar applications," Proc. SPIE **3945**, 98–105 (2000).
4. G. J. Koch, "Automatic laser frequency locking to gas absorption lines," Opt. Eng. **42**, 1690–1693 (2003).
5. G. Poberaj, A. Fix, A. Assion, M. Wirth, C. Kiemle, and G. Ehret, "Airborne all-solid-state DIAL for water vapour measurements in the tropopause region: system description and assessment of accuracy," Appl. Phys. B **75**, 165–172 (2002).
6. H.-M. Fang, S.-C. Wang, and J.-T. Shy, "Frequency stabilization of an external cavity diode laser to molecular iodine at 657.483 nm," Appl. Opt. **45**, 3173–3176 (2006).
7. J. M. Supplee, E. A. Whittaker, and W. Lenth, "Theoretical description of frequency modulation and wavelength modulation spectroscopy," Appl. Opt. **33**, 6294–6302 (1994).
8. S. Schilt, L. Thévenaz, and P. Robert, "Wavelength modulation spectroscopy: combined frequency and intensity laser modulation," Appl. Opt. **42**, 6728–6738 (2003).
9. R. Matthey, S. Schilt, D. Werner, C. Affolderbach, L. Thévenaz, and G. Mileti , "Diode laser frequency stabilisation for water-vapour differential absorption sensing," Appl. Phys. B. **85**, 477–485 (2006).
10. G. Santarelli, A. Clairo, S. N. Lea, and G. M. Tino, "Heterodyne optical phase-locking of extended-cavity semiconductor lasers at 9 GHz," Opt. Commun. **104**, 339–344 (1994).
11. U. Gliese, T. N. Nielsen, M. Bruun, E. L. Christensen, K. E. Stubkjaer, S. Lindgren, and B. Broberg, "A wideband heterodyne optical phase-lock loop for generation of 3–18 GHz microwave carriers," IEEE Photon. Technol. Lett. **4**, 936–938 (1992).
12. G. Ritt, G. Cennini, C. Geckeler, and M. Weitz, "Laser frequency offset locking using a side of filter technique," Appl. Phys. B. **79**, 363–365 (2004).
13. P. Kluczynski, J. Gustafsson, A. M. Lindberg, and O. Axner, "Wavelength modulation absorption spectrometry—an extensive scrutiny of the generation of signals," Spectrochim. Acta B **56**, 1277–1354 (2001).
14. C. Affolderbach and G. Mileti, "A compact laser head with high-frequency stability for Rb atomic clocks and optical instrumentation," Rev. Sci. Instrum. **76**, 073108 (2005).
15. S. Schilt and L. Thévenaz, "Experimental method based on wavelength-modulation spectroscopy for the characterization of semiconductor lasers under direct modulation," Appl. Opt. **43**, 4446–4453 (2004).
16. D. S. Bomse, A. C. Stanton, and J. A. Silver, "Frequency modulation and wavelength modulation spectroscopies: comparison of experimental methods using a lead-salt diode laser," Appl. Opt. **31**, 718–731 (1992).